THE JOURNAL OF PHYSICAL CHEMISTRY C

Article

pubs.acs.org/JPCC

Modulation of Photocarrier Dynamics in Indoline Dye-Modified TiO_2 Nanorod Array/P3HT Hybrid Solar Cell with 4-*tert*-Butylpridine

Shu-Chien Hsu, Wen-Pin Liao, Wan-Hsien Lin, and Jih-Jen Wu*

Department of Chemical Engineering, National Cheng Kung University, Tainan 701, Taiwan

Supporting Information

ABSTRACT: The influences of the 4-*tert*-butylpridine (TBP) treatment prior to the P3HT infiltration on the performance of the D149-modified TiO_2 nanorod (NR) array/P3HT solar cell are investigated in this work. The efficiency of the D149-modified TiO_2 NR array/P3HT hybrid solar cell is enhanced from 1.58% to 1.83% through the TBP treatment for a proper duration. With the cell characteristic of both D149 and P3HT contributing to the photocurrent, the short-circuit current density of the hybrid solar cell is enhanced by 30% with the TBP treatment. Absorption spectra indicate desorption of D149 molecules from TiO_2 NRs with TBP treatment, suggesting that part of the TiO_2 NR surface is passive by TBP molecules. Time-resolved photoluminescence and electrochemical impedance spectroscopy are employed to investigate the photocarrier dynamics of the hybrids. The results indicate that the photocarrier dynamics are modulated to decrease both the photocarrier generation rate and the recombination rate at the interface of D149-modified TiO_2 NR and P3HT when TBP molecules are adsorbed on TiO_2 NRs after the treatment. The enrichment of the photocurrent in the D149-modified TiO_2 NR array/P3HT hybrid solar cell is, therefore, achievable with an appropriate ratio of D149 and TBP coadsorbed on the TiO_2 NR array.

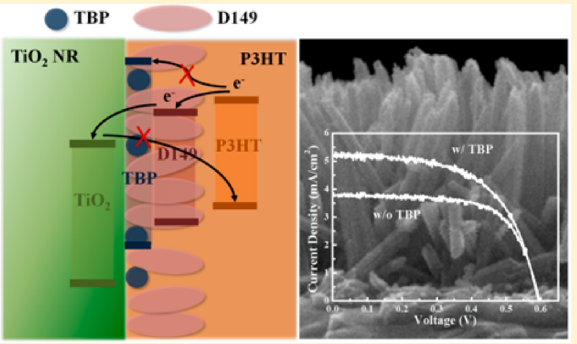

INTRODUCTION

Hybrid polymer solar cells, which are fabricated by blending inorganic oxide nanoparticles (NPs) with conjugated polymer, have attracted considerable attention because of the good stability and low cost of the oxide NPs.[1−3] However, the characteristic of poor carrier transport, which is similar to the organic bulk heterojunction (BHJ), limits the performance of the hybrid solar cell.[1,4] It is attributed to insufficient connection between NPs. Therefore, a photovoltaic device structure composed of a direct and ordered path facilitating electron transport to the collecting electrode is suggested to improve the performance of the hybrid polymer solar cells.[1,5] One-dimensional metal oxide nanostructures, such as nanorod (NR) and nanotube arrays, grown on electrodes have been employed as the ordered electron acceptors/transporters.[6−8] The conjugated polymers are then infiltrated into the free spaces of the order nanostructures to form the hybrid active layers. This device configuration with the ordered electron acceptors/transporters also offers the potential to improve hole mobility.[1] However, poor charge separation and significant charge recombination, which restrict the cells to high efficiencies, are observed in the hybrid solar cells. It is mainly ascribed to the chemical incompatibility between polymer and inorganic nanostructures. The organic dye molecules have been utilized to improve the interfacial morphology of the hybrid solar cells.[6,9−11] In addition to being an interfacial modifier, the dye molecule may also contribute to the photocurrent of the hybrid solar cell with an appropriate interfacial energetic.[6,9]

4-*tert*-Butylpridine (TBP) has been employed as an electrolyte additive in dye-sensitized solar cells (DSSCs).[12,13] The anode surface that is uncovered by the dye will be passive by the adsorption of TBP molecules.[14] Moreover, the TBP molecule forms a complex with iodine in the electrolyte.[15] The addition of TBP in the electrolyte can elevate the conduction band edge of the anode and suppress the charge recombination of injected electrons with oxidized species in the electrolyte, resulting in the increase of the open-circuit voltage (V_{oc}).[13,16] However, the electron injection dynamic is also influenced by the shift of the conduction band edge in some dye-sensitized photoanodes. The short-circuit photocurrent density (J_{sc}), therefore, shows a correlation with the TBP concentration in the electrolyte.[13] It has been reported that the performance of the organic dye-modified nanoporous TiO_2−P3HT hybrid solar cell can also be influenced by the Li salt and TBP treatment prior to the deposition of P3HT.[9] Without the treatment, the photocurrent and efficiency of the cell that performs as a solid-state DSSC are very poor. A remarkable enhancement of the cell efficiency is achieved by the treatment, resulting from that the energy level of the interfacial modifying

Received: September 20, 2012
Revised: November 10, 2012
Published: November 20, 2012

dye was shifted to make P3HT contribute to the photocurrent as well. In this case, however, it was concluded that Li-salt treatment was essential for improved cell performance.

We have demonstrated that the performance of the rutile TiO_2 nanoarchitecture array/P3HT hybrid solar cell is significantly improved through interfacial modification with the D149 dye molecule.[10] The D149 molecule not only provides an appropriate band alignment in between the P3HT/TiO_2 nanoarchitecture array but also improves the compatibility of the interface morphology of the hybrid. Charge separation and electron lifetime are, therefore, improved in the D149-modified TiO_2 NRs/P3HT hybrid solar cells, resulting in the enrichments of the cell performances. With the cell characteristic that both D149 and P3HT contribute to the photocurrent, the influences of the TBP treatment (in the absence of Li salt) prior to the P3HT infiltration on the performance of the D149-modified TiO_2 NR array/P3HT solar cell are investigated in this work. Improvement of photovoltaic performance of the D149-modified TiO_2 NR array/P3HT hybrid solar cell is attained through the TBP treatment for a proper duration. The energy band diagram of the TBP-treated hybrid active layer at equilibrium is constructed using cyclic voltammetry (CV), Kelvin probe force microscopy (KPM), and optical absorption measurements. Time-resolved photoluminescence (TRPL) and electrochemical impedance spectroscopy (EIS) measurements are employed to investigate the dynamics of charge separation and recombination in the D149-modified ordered hybrid solar cells. The results indicate that TBP molecules coadsorbed on the D149-modified TiO_2 NR array play a crucial role in modulating the photocarrier dynamics in the D149-modified TiO_2 NR array/P3HT hybrid solar cell.

EXPERIMENTAL SECTION

Aligned TiO_2 NR arrays were hydrothermally grown on the fluorine-doped tin oxide (FTO) substrate in 40 mL of aqueous hydrochloric acid (the ratio of DI water to 37% HCl is 1:1) and 0.7 mL of titanium(IV) *tert-n*-butoxide (TnBT) at 150 °C.[10,17,18] The NR array/FTO substrate was further immersed in an aqueous solution of 0.1 M $TiCl_4$ at 50 °C for 1 h, followed by heat treatment at 450 °C for 30 min to synthesize NPs on the surfaces of the NRs. The morphology of the TiO_2 NR array, as shown in Figure 1a, was examined using scanning electron microscopy (SEM, JEOL JSM-7000F).

D149 dye adsorptions were carried out by immersing the TiO_2 NR arrays in a 0.5 mM acetonitrile/*t*-butanol (1:1) solution of D149 dye at 70 °C for 1 h. TBP treatments of the dye-modified TiO_2 NR array were further conducted in a 60 mg/mL acetonitrile solution of TBP at room temperature. Optical absorptions of the modified TiO_2 NR arrays were measured using a UV−vis-IR spectrophotometer (JASCO V-670). P3HT infiltration into the TiO_2 NR array was carried out in a glovebox. The TiO_2 NR array wetted with *p*-xylene was covered with a 45 mg/mL chlorobenzene solution of P3HT (Sigma-Aldrich, M_w = 80 000) and was then spun to form a thin layer of P3HT on the TiO_2 NR array/P3HT hybrid. A heat treatment was immediately performed at 150 °C for 20 min. For simplicity, the hybrids fabricated using D149-modified TiO_2 NR arrays with TBP treatments for 0.5, 1, 2, and 2.5 min, respectively, prior to P3HT infiltration are named as TBP-0.5, TBP-1, TBP-2, and TBP-2.5 hybrids hereafter. The CV measurements were performed in acetonitrile solution containing the supporting electrolyte of tetrabutylammonium hexafluorophosphate ($TBAPF_6$, 0.1 M). The modified TiO_2 NR array or P3HT infiltrated TiO_2 NR array, a platinum wire, and a nonaqueous $Ag/AgNO_3$ electrode (0.56 V vs NHE) were used as the working, counter, and reference electrodes, respectively. The work functions of the hybrids were measured using Kelvin probe force microscopy (KPM, Veeco Innova).

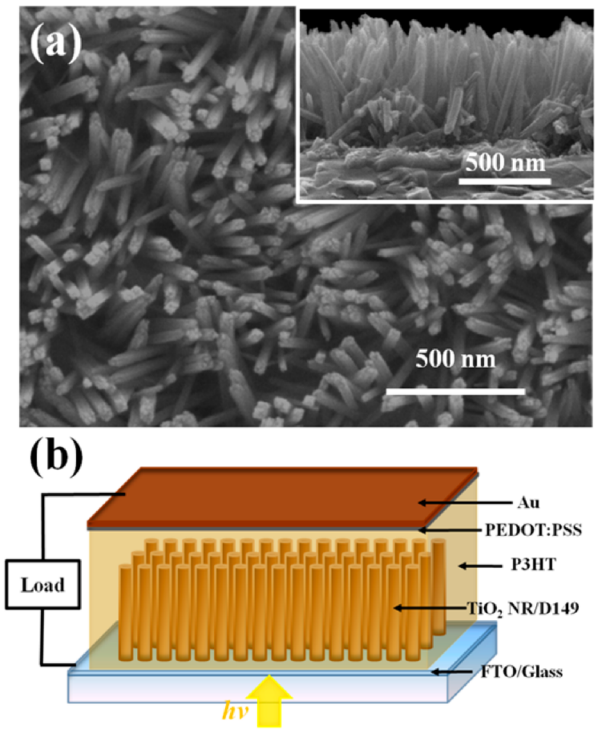

Figure 1. (a) Top view and cross-sectional view (inset) SEM images of the TiO_2 NR array. (b) Schematic of the D149-modified TiO_2 NR array/P3HT hybrid solar cell.

TiO_2 NR array/P3HT hybrid solar cells with island-type electrodes[19] were fabricated in this work. A thin layer of PEDOT:PSS (Baytron PVP AI 4083) was spun on the TiO_2 NR array/P3HT hybrid. Finally, a 100 nm thick gold film was deposited on the top of the PEDOT:PSS layer. The schematic of the modified TiO_2 NR array/P3HT hybrid solar cell is shown in Figure 1b. A black-painted mask on the FTO substrate side was used to create an exposed area of 0.03 cm^2 for all hybrid solar cells. Photovoltaic characteristics of the hybrid solar cells were measured under AM 1.5 simulated sunlight at 100 mW cm^{-2} (300 W, model 91160A, Oriel).

Time-resolved photoluminescence (TRPL) spectroscopy measurements (integrated by Preotrustech Co., Ltd.) were conducted using a pulse laser (405 nm) with a pulse width of 75 ps for excitation. The TRPL decays at 710 nm were recorded by a time-correlated single-photon counting (TCSPC) spectrometer. Electrochemical impedance spectroscopy (EIS) measurements were performed under the illumination of a green LED light (530 nm) with various intensities by applying a 10 mV ac signal over the frequency range of $1-10^5$ Hz at the V_{oc} of the hybrid solar cells using a potentiostat with a frequency response analyzer (FRA, Zaher, IM6ex). A two-channel transmission line model was employed to investigate the electron transport and recombination in the hybrid solar cells.[10,20]

RESULTS AND DISCUSSION

The influences of the TBP treatment on the performance of the D149-modified TiO_2 NR array/P3HT solar cell are investigated by varying the treatment periods. Figure 2 shows the $J-V$ curves of the hybrid solar cells fabricated using D149-modified TiO_2 NR arrays with the TBP treatment for 0–2.5 min prior to the P3HT infiltration. The photovoltaic parameters of the five cells are summarized in Table 1. It reveals that the short-circuit current density (J_{sc}) is increased while the fill factor (FF) is reduced when the TBP treatment period is prolonged from 0 to 2 min. Moreover, with the TBP treatment for less than 2 min, the open-circuit voltages (V_{oc}) of the D149-modified TiO_2 NR array/P3HT cells are comparable to the one without treatment (TBP-0 solar cell). Combining the influences on J_{sc} and FF, as shown in Table 1, the efficiency of the TBP-0.5 solar cell is slightly lower than that of the TBP-0 solar cell. When the TBP treatment period is prolonged further, the efficiency of the D149-modified TiO_2 NR array/P3HT cell is improved, which is mainly ascribed to the enhancement of J_{sc}. The J_{sc} of the hybrid solar cell is dramatically enhanced by 30% in the TBP-2 solar cell. Compared to the TBP-0 solar cell, the efficiency of the D149-modified TiO_2 NR array/P3HT solar cell is, therefore, improved from 1.58% to 1.83% through the 2 min TBP treatment of the D149-modified TiO_2 NR array prior to the P3HT infiltration. On the other hand, when the TBP treatment period is increased to 2.5 min, the efficiency of the TBP-2.5 solar cell becomes inferior to that of TBP-0, which is pertaining to the significant reductions of V_{oc} and FF.

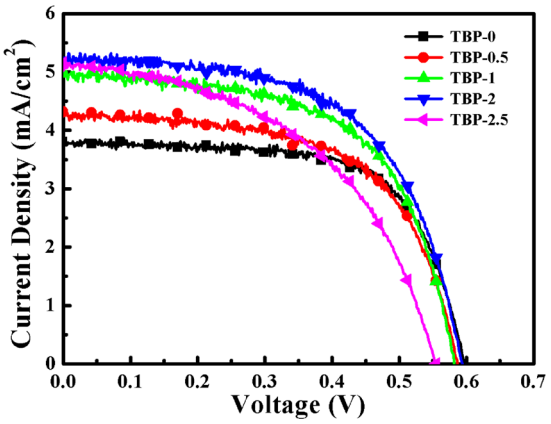

Figure 2. $J-V$ curves of D149-modified TiO_2 NR array/P3HT solar cells with TBP treatment. The TBP treatment periods are from 0 to 2.5 min.

Table 1. Photovoltaic Parameters of D149-Modified TiO_2 NR Array/P3HT Solar Cells with TBP Treatments

D149-modified TiO_2/P3HT cell	V_{oc} (V)	J_{sc} (mA/cm^2)	FF	η (%)
TBP-0	0.60	3.93	0.67	1.58
TBP-0.5	0.59	4.27	0.62	1.55
TBP-1	0.58	4.95	0.60	1.74
TBP-2	0.59	5.18	0.59	1.83
TBP-2.5	0.55	5.08	0.49	1.39

It has been reported that, in DSSCs, TBP molecules in the electrolyte will bleach the D149-sensitized photoanode due to dye desorption.[21] Figure 3 shows the absorption spectra of the D149-modified TiO_2 NR arrays without and with TBP treatment for 2 min. The absorption peaks in the range of 450–650 nm are obtained in the spectra of both D149-modified TiO_2 NR arrays. However, the intensity of the absorption peak is obviously reduced after the 2 min TBP treatment. The dye desorption from the D149-modified TiO_2 NR array after the TBP treatment is also observed in this work, and the amount of D149 on the TiO_2 NR array is estimated to be decreased from 5.1 to 3.7 nmol cm^{-2}. It has been evidenced that TBP molecules can bind at the TiO_2 surface.[22] We, therefore, suggest that D149 and TBP molecules are coadsorbed on the TiO_2 NR array after the TBP treatment.

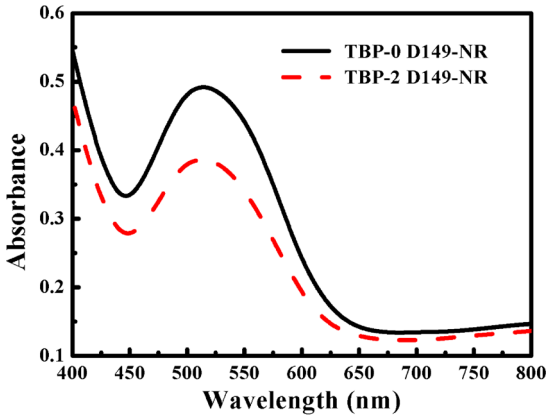

Figure 3. UV–vis absorption spectra of D149-modied TiO_2 NR arrays without and with TBP treatment for 2 min.

Photocurrent generation mechanisms in the D149-modified TiO_2 NR/P3HT hybrid solar cells have been examined by the band diagrams of the hybrids at equilibrium and TRPL measurements in our previous work.[10] It was concluded that both D149 molecules and P3HT are able to contribute to photocurrents in the D149-modified TiO_2 NR array/P3HT hybrid solar cells. As aforementioned, the J_{sc} of the D149-modified TiO_2 NR array/P3HT hybrid solar cell is improved, although the amount of the D149 adsorbed on the TiO_2 NR array is reduced with the TBP treatment prior to the P3HT infiltration. To investigate the influences of TBP treatment on the photocurrent generation mechanisms in the D149-modified TiO_2 NR/P3HT hybrid solar cells, the band diagram of the TBP-2 hybrid at equilibrium is first constructed in the present work.

The method for construction of the band diagram of the TiO_2 NR array/D149/P3HT hybrid at equilibrium has been demonstrated in our previous work in detail.[10] To estimate the HOMO energy levels of the D149 in the hybrids at equilibrium, the TiO_2 NR array/D149/P3HT hybrids are employed to be working electrodes for the CV measurements. The CV results of the TBP-0 and TBP-2 hybrids are shown in Figure 4a. For comparison, the CV result of the TiO_2 NR array/P3HT hybrid is also displayed in the figure. The oxidation onset potential (E_{onset}) of the three hybrids are in the order of TBP-0 hybrid > TBP-2 hybrid > TiO_2 NR array/P3HT hybrid. As the D149-modified TiO_2 NR array is treated with TBP prior to the P3HT infiltration, the E_{onset} of the TiO_2 NR array/D149/P3HT hybrid is negatively increased toward that of TiO_2 NR array/P3HT, which is correlated to the reduction of the amount of D149 adsorption on the TiO_2 NR array after the TBP treatment for 2 min. The HOMO energy levels (E_{HOMO}) of D149, TBP, and P3HT, which are determined using CV measurement, are in the order of P3HT > D149 > TBP (Figure

dx.doi.org/10.1021/jp309328p | J. Phys. Chem. C 2012, 116, 25721–25726

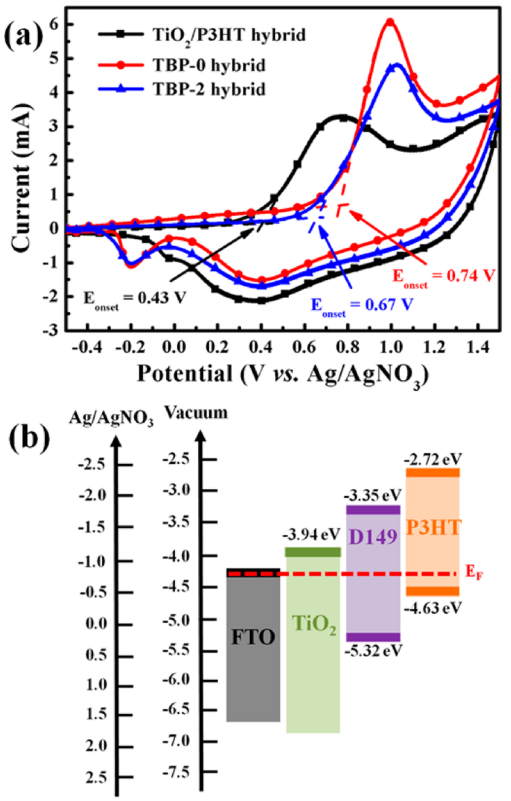

Figure 4. (a) CV results of the TiO_2 NR array/P3HT hybrid as well as the D149-modified TiO_2 NR array/P3HT hybrid without and with TBP treatment for 2 min. (b) Equilibrium energy band diagram of the D149-modified TiO_2 NR array/P3HT hybrid with TBP treatment for 2 min.

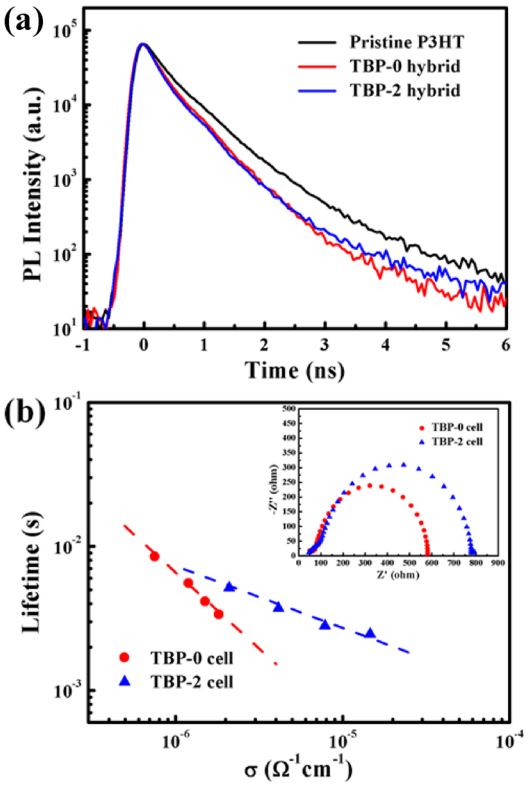

Figure 5. (a) TRPL spectra of pristine P3HT as well as D149-modified TiO_2 NR array/P3HT hybrid films with and without TBP treatment for 2 min. (b) Conductivity dependence of electron lifetimes in D149-modified TiO_2 NR array/P3HT hybrid cells with and without TBP treatment for 2 min. Nyquist plots (inset) of D149-modified TiO_2 NR array/P3HT hybrid cells with and without TBP treatment for 2 min.

S1 and Table S1, Supporting Information). Because the TBP-2 hybrid is composed of the D149 and TBP comodified TiO_2 NR array and the infiltrated P3HT, the electron from electrolyte to FTO should follow the transport pathway of LUMO of P3HT → LUMO of D149 → CB edge of TiO_2 → Fermi level of FTO for obtaining the anodic current during CV measurement. The E_{onset} obtained from the CV result is attributed to the oxidation of the D149 molecule due to its lowest E_{HOMO} in the whole electron transport pathway.[9] Consequently, the E_{HOMO} of D149 in the TiO_2 NR array/D149/P3HT hybrids at equilibrium can be determined using the E_{onset}, as shown in Figure 4a.

On the other hand, the E_{HOMO} of P3HT in the hybrid at equilibrium is estimated from the work function of the TiO_2 NR array/D149/P3HT hybrid ($E_{W,hybrid}$).[10] $E_{W,hybrid}$ is measured by KPM and is calibrated by the offset between CV and KPM measurements. The LUMO energy levels of the D149 and P3HT are then obtained by adding up the corresponding band-gap energies of 1.97 and 1.91 eV, which are determined by adsorption spectra.[10] The resultant band diagram of the TBP-2 hybrid at equilibrium is shown in Figure 4b. It reveals that both D149 and P3HT are able to contribute to the photocurrent in the TBP-2 solar cell, which is similar to the characteristic of the TBP-0 solar cell.[10] The equilibrium energy band diagram of the TBP-2 hybrid confirms that the cell is not a solid-state dye-sensitized solar cell.

To further examine the functions of the TBP, TRPL and EIS were, respectively, employed to investigate the dynamics of charge separation and recombination at the interface between TiO_2 NR and P3HT in the hybrid solar cells. Figure 5a shows the TRPL decay curves of the pristine P3HT as well as TBP-0 and TBP-2 hybrids on FTO substrates. The instrument response function is first eliminated from the decay curves, and the decays are subsequently analyzed by biexponential decay kinetics.[23] The average PL lifetimes of the pristine P3HT as well as TBP-0 and TBP-2 hybrids are 580, 416, and 437 ps, respectively. Compared to the pristine P3HT, charge separation is enhanced in the TBP-0 hybrid by showing a shorter PL lifetime, which is attributed to the presence of the D149-modified TiO_2 NR array. We have demonstrated that D149 molecules perform well as an efficient electronic mediator to enhance charge separations at the P3HT/TiO_2 interfaces.[10] When the D149-modified TiO_2 NR array is treated with TBP for 2 min prior to the P3HT infiltration, the average PL lifetime in the TBP-2 hybrid is still shorter than that in the pristine P3HT. It indicates that P3HT does contribute to the photocurrent in the TBP-2 solar cell as the predication of the band diagram of the TBP-2 hybrid at equilibrium shown in Figure 4b. However, the longer PL lifetime in the TBP-2 hybrid than that in the TBP-0 hybrid is observed, indicating that charge separation at the interface of P3HT and the D149-modified TiO_2 NR is slightly suppressed by the TBP treatment. Considering the reduction of photocurrent contributed from both D149 and P3HT, the significant enrichment of the J_{sc} in the TBP-2 solar cell should be dominated by the other function of TBP.

Figure 5b displays the dynamics of charge recombination at the interface of TiO_2 NR and P3HT in the TBP-0 and TBP-2

dx.doi.org/10.1021/jp309328p | J. Phys. Chem. C 2012, 116, 25721−25726

solar cells, which are determined by EIS measurement at V_{oc} under various light intensities of a green light (530 nm) illumination. The electron lifetimes (τ_n) in the two D149-modified TiO_2 NR array/P3HT solar cells are represented as functions of conductivity (σ) in the electron acceptors of TiO_2 NRs.[20] Conductivities of the TiO_2 NRs can be estimated by the cell geometrical parameters and the electron transport resistance in the TiO_2 NRs extracted from the EIS data.[20] It shows that the electron lifetime in the TBP-2 solar cell is longer than that in the TBP-0 cell under the same conductivity, that is, the condition of the TiO_2 NRs filled with the same amount of photoelectrons. The result indicates that the interfacial recombination in the D149-modified TiO_2 NR array/P3HT solar cell is suppressed when the D149-modified TiO_2 NR array is treated with TBP for 2 min prior to the P3HT infiltration. We have demonstrated that D149 molecules at the interface between TiO_2 NRs and P3HT serve as an effective recombination barrier to enhance the electron lifetime in the TiO_2 NRs.[10] In the present work, the EIS results indicate that the TBP molecules play a crucial role in further prevention of the interfacial recombination, resulting in that the TBP-2 solar cell with coadsorbed TBP and D149 molecules at the TiO_2 NR/P3HT interfaces possesses a larger recombination resistance compared to the TBP-0 solar cell with D149 molecules alone.

As aforementioned, the active layer consists of a D149 and TBP comodified TiO_2 NR array infiltrated with P3HT in the TBP-2 solar cell. Figure 6 shows the schematic of photocarrier

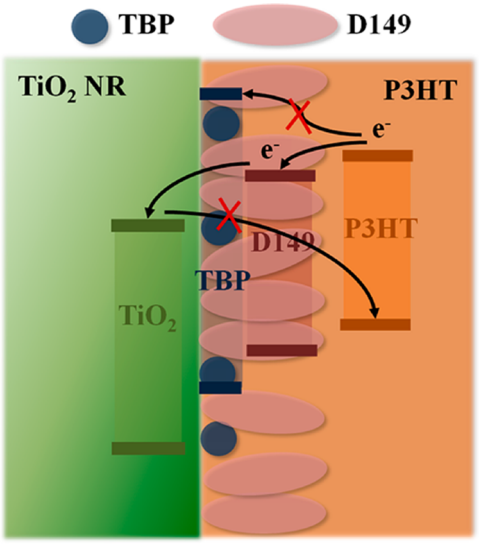

Figure 6. Schematic of photocarrier dynamics at the interface between TiO_2 NR and P3HT with the modification of D149 and TBP.

dynamics at the interface between TiO_2 NR and P3HT with the modification of D149 and TBP. Compared to the one without TBP treatment, the photocurrent attributed to D149 molecules should be less in the TBP-treated solar cell. In addition, dye molecules perform well as an efficient electronic mediator at the P3HT/TiO_2 interface to improve the electron injection from P3HT to TiO_2.[10] The TRPL results in Figure 5a reveal that the effective charge separation behavior at the interface of P3HT and TiO_2 modified by D149 molecules is further modulated by the coadsorbed TBP molecules. A longer PL average lifetime is observed in the TBP-treated hybrid. The interfaces of P3HT and TiO_2 where TBP molecules adsorbed on may not facilitate exciton dissociation, whereas charge separation still efficiently occurs at where D149 molecules adsorbed on, as illustrated in Figure 6. The effective interfacial area for charge separation in the D149-modified TiO_2 NR/P3HT solar cells is, therefore, slightly reduced with the presence of TBP at interfaces, resulting in the reduction of photogenerated electrons into the TiO_2 NR array from P3HT. As discussed above, the carrier generation rate from both D149 and P3HT in the TBP-treated cell will be less than that in the one without TBP treatment.

On the other hand, EIS results indicate that the interfacial recombination resistance in the D149-modified TiO_2 NR/P3HT solar cells is enhanced with the TBP treatment, as shown in Figure 5b. We suggest that the coadsorbed TBP molecules possessing an insulating character block some electrons from the CB edge of TiO_2 back to the HOMO level of P3HT, as illustrated in Figure 6, which can significantly reduce the interfacial recombination rate and, therefore, enhance the electron lifetime in the TiO_2 NRs. With an identical interface area provided by the TiO_2 NR array, the interfacial modification of the TiO_2 NR/P3HT hybrid with D149 molecules improves the interface morphology, which is attributed to not only an appropriate band alignment of dye in between P3HT/TiO_2 NR but also the improved compatibility of the interface morphology of the hybrid.[10] When the interface between D149-modified TiO_2 NR and P3HT is further treated with TBP molecules, that is, some D149 molecules are replaced by TBP molecules at the interface, the photocarrier dynamics are modulated to decrease both the photocarrier generation rate and the recombination rate at the interface of TiO_2 NR and P3HT. The enrichment of the photocurrent in the D149-modified TiO_2 NR array/P3HT hybrid solar cell is, therefore, achievable with an appropriate ratio of D149 and TBP adsorbed on the TiO_2 NR array.

The maximum V_{oc} of the dye-modified TiO_2 NR array–P3HT solar cell is determined by the potential difference of the Fermi levels of dye-modified TiO_2 NR and P3HT before Fermi level alignment. As listed in Table S2 (Supporting Information) KPM measurements show that the work function of the D149-modified TiO_2 NR is enlarged with TBP treatment, indicating that the Fermi level of the D149-modified TiO_2 NR is lowered when some D149 molecules on the TiO_2 surface are replaced with TBP. On the other hand, the EIS measurements reveal that the TiO_2 NR/P3HT interface with both TBP and D149 molecules possesses a larger recombination resistance compared with the one with D149 molecules alone. The lowering of the Fermi level of D149-modified TiO_2 NR and the enlarged recombination resistance are simultaneously observed in the TBP-treated cell, which may result in the comparable V_{oc} in the D149-modified TiO_2 NR/P3HT solar cells without and without the TBP treatment. Therefore, a significantly enriched J_{sc}, an accompanying comparable V_{oc}, and a slightly decreased FF are attained by modulating the photocarrier dynamics at the interface through replacing some D149 molecules with TBP ones in the D149-modified TiO_2 NR/P3HT solar cell. As a result, the efficiency of the dye-modified TiO_2 NR/P3HT hybrid solar cell can be improved by the TBP treatment.

CONCLUSIONS

The efficiency of the D149-modified TiO_2 NR array/P3HT hybrid solar cell is enhanced from 1.58% to 1.83% through the TBP treatment for 2 min. J_{sc} is enhanced by 30%, while a comparable V_{oc} and a decreased FF are obtained in the TBP-2

solar cell. The equilibrium energy band diagram of the TBP-treated hybrid constructed in this work reveals that both D149 and P3HT are able to contribute to the photocurrent in the solar cell. However, the dye desorption from the D149-modified TiO_2 NR array after the TBP treatment is observed from the absorption spectra. We found that the TBP plays a crucial role in the modulation of the photocarrier dynamics at the interface of the D149-modified TiO_2 NR and P3HT through replacing some D149 molecules. TRPL measurements show that charge separation at the interface of P3HT and D149-modified TiO_2 NR is slightly suppressed by the TBP treatment. The reduction of the photocurrent contributed from both D149 and P3HT in the TBP-treated solar cell is observed. Nevertheless, EIS results indicate that the interfacial recombination resistance in the D149-modified TiO_2 NR/P3HT solar cells is enhanced with the TBP treatment. When the interface between D149-modified TiO_2 NR and P3HT is treated with TBP molecules, that is, some D149 molecules are replaced by TBP molecules at the interface, the photocarrier dynamics are modulated to decrease both the photocarrier generation rate and the recombination rate at the interface of TiO_2 NR and P3HT. The enrichment of the photocurrent in the D149-modified TiO_2 NR array/P3HT hybrid solar cell is, therefore, achievable with an appropriate ratio of D149 and TBP adsorbed on the TiO_2 NR array. On the other hand, KPM characterizations show that the Fermi level of D149-modified TiO_2 NR is lowered after TBP treatment. Combining the lowered Fermi level and the enlarged recombination resistance, the V_{oc} in the TBP-treated solar cell is comparable to that in the one without treatment. Therefore, the improved efficiency of the D149-modified TiO_2 NR array/P3HT hybrid solar cell, as a result of a significantly enriched J_{sc}, an accompanying comparable V_{oc}, and a slightly decreased FF, is attained by modulating the photocarrier dynamics at the interface through replacing some D149 molecules with TBP in the D149-modified TiO_2 NR/P3HT solar cell.

■ ASSOCIATED CONTENT

Ⓢ Supporting Information

CV results of P3HT, D149, and TBP absorbed on TiO_2 NR arrays; HOMO energy level positions of P3HT, D149, and TBP absorbed on TiO_2 NR arrays; and work functions of D149-modified TiO_2 NR arrays with and without TBP treatment determined by KPM measurements. This material is available free of charge via the Internet at http://pubs.acs.org.

■ AUTHOR INFORMATION

Corresponding Author

*E-mail: wujj@mail.ncku.edu.tw. Fax: +886 6234 4496. Tel: +886 6275 7575, ext. 62694.

Notes

The authors declare no competing financial interest.

■ ACKNOWLEDGMENTS

The financial support from the National Science Council in Taiwan under Contract Nos. NSC 99-2221-E-006-198-MY3 and NSC 100-2628-E006-032-MY2 is gratefully acknowledged.

■ REFERENCES

(1) Mayer, A. C.; Scully, S. R.; Hardin, B. E.; Rowell, M. W.; McGehee, M. D. *Mater. Today* **2007**, *10*, 28.
(2) Gunes, S.; Neugebauer, H.; Sariciftci, N. S. *Chem. Rev.* **2007**, *107*, 1324.
(3) Chen, W.; Nikiforov, M. P.; Darling, S. B. *Energy Environ. Sci.* **2012**, *5*, 8045.
(4) Saunders, B. R.; Turner, M. L. *Adv. Colloid Interface Sci.* **2008**, *138*, 1.
(5) Tepavcevic, S.; Darling, S. B.; Dimitrijevic, N. M.; Rajh, T.; Sibener, S. J. *Small* **2009**, *5*, 1776.
(6) Mor, G. K.; Kim, S.; Paulose, M.; Varghese, O. K.; Shankar, K.; Basham, J.; Grimes, C. A. *Nano Lett.* **2009**, *9*, 4250.
(7) Lee, Y.-J.; Lloyd, M. T.; Olson, D. C.; Grubbs, R. K.; Lu, P.; Davis, R. J.; Voigt, J. A.; Hsu, J. W. P. *J. Phys. Chem. C* **2009**, *113*, 15778.
(8) Sung, Y.-H.; Liao, W.-P.; Chen, D.-W.; Wu, C.-T.; Chang, G.-J.; Wu, J.-J. *Adv. Funct. Mater.* **2012**, *22*, 3808.
(9) Zhu, R.; Jiang, C.-Y.; Liu, B.; Ramakrishna, S. *Adv. Mater.* **2009**, *21*, 994.
(10) Liao, W.-P.; Hsu, S.-C.; Lin, W.-H.; Wu, J.-J. *J. Phys. Chem. C* **2012**, *116*, 15938.
(11) Moon, S.-J.; Baranoff, E.; Zakeeruddin, S. M.; Yeh, C.-Y.; Diau, E. W.-G.; Gratzel, M.; Sivula, K. *Chem. Commun.* **2011**, *47*, 8244.
(12) Huang, S. Y.; Schlichthörl, G.; Nozik, A. J.; Grätzel, M.; Frank, A. J. *J. Phys. Chem. B* **1997**, *101*, 2576.
(13) Koops, S. E.; O'Regan, B. C.; Barnes, P. R. F.; Durrant, J. R. *J. Am. Chem. Soc.* **2009**, *131*, 4808.
(14) Nazeeruddin, M. K.; Kay, A.; Rodicio, I.; Humphry-Baker, R.; Mueller, E.; Liska, P.; Vlachopoulos, N.; Graetzel, M. *J. Am. Chem. Soc.* **1993**, *115*, 6382.
(15) Boschloo, G.; Häggman, L.; Hagfeldt, A. *J. Phys. Chem. B* **2006**, *110*, 13144.
(16) Schlichthörl, G.; Huang, S. Y.; Sprague, J.; Frank, A. J. *J. Phys. Chem. B* **1997**, *101*, 8141.
(17) Liu, B.; Aydil, E. S. *J. Am. Chem. Soc.* **2009**, *131*, 3985.
(18) Liao, W.-P.; Wu, J.-J. *J. Mater. Chem.* **2011**, *21*, 9255.
(19) Kim, M. S.; Kang, M. G.; Guo, L. J.; Kim, J. *Appl. Phys. Lett.* **2008**, *92*, 133301.
(20) Fabregat-Santiago, F.; Bisquert, J.; Cevey, L.; Chen, P.; Wang, M.; Zakeeruddin, S. M.; Grätzel, M. *J. Am. Chem. Soc.* **2008**, *131*, 558.
(21) Le Bahers, T.; Labat, F.; Pauporte, T.; Ciofini, I. *Phys. Chem. Chem. Phys.* **2010**, *12*, 14710.
(22) Shi, C.; Dai, S.; Wang, K.; Pan, X.; Kong, F.; Hu, L. *Vib. Spectrosc.* **2005**, *39*, 99.
(23) Jarzab, D.; Szendrei, K.; Yarema, M.; Pichler, S.; Heiss, W.; Loi, M. A. *Adv. Funct. Mater.* **2011**, *21*, 1988.